Optics Letters

High-temperature strain sensor based on sapphire fiber Bragg grating

JUN HE,[1,2,3] ZHUODA LI,[1,2] XIZHEN XU,[1,2,3,*] QINGMING TAN,[1,2] XIAOYU WENG,[1] LIWEI LIU,[1] JUNLE QU,[1] CHANGRUI LIAO,[1,2,3] AND YIPING WANG[1,2,3]

[1]State Key Laboratory of Radio Frequency Heterogeneous Integration, Key Laboratory of Optoelectronic Devices and Systems of Ministry of Education/Guangdong Province, College of Physics and Optoelectronic Engineering, Shenzhen University, Shenzhen 518060, China
[2]Shenzhen Key Laboratory of Ultrafast Laser Micro/Nano Manufacturing, Guangdong and Hong Kong Joint Research Centre for Optical Fibre Sensors, Shenzhen University, Shenzhen 518060, China
[3]Guangdong Laboratory of Artificial Intelligence and Digital Economy (SZ), Shenzhen 518107, China
*xizhenxu@szu.edu.cn

Received 16 October 2023; revised 10 December 2023; accepted 12 December 2023; posted 15 December 2023; published 14 January 2024

Sapphire fiber Bragg grating (SFBG) is a promising high-temperature strain sensor due to its melting point of 2045°C. However, the study on the long-term stability of SFBG under high temperature with an applied strain is still missing. In this paper, we reported for the first time to our knowledge on the critical temperature point of plastic deformation of the SFBG and demonstrated that the SFBG strain sensor can operate stably below 1200°C. At first, we experimentally investigated the topography and the spectral characteristics of the SFBG at different temperatures (i.e., 25°C, 1180°C, and 1600°C) with applied 650 µε. The reflection peak of the SFBG exhibits a redshift of about 15 nm and broadens gradually within 8 h at 1600°C, and the tensile force value decreases by 0.60 N in this process. After the test, the diameter of the SFBG region decreases from 100 to 88.6 µm, and the grating period is extended from 1.76 to 1.79 µm. This indicates that the plastic deformation of the SFBG happened indeed, and it was elongated irreversibly. Moreover, the stability of the Bragg wavelength of the SFBG under high temperature with the applied strain was evaluated. The result demonstrates the SFBG can be used to measure strain reliably below 1200°C. Furthermore, the strain experiments of SFBG at 25°C, 800°C, and 1100°C have been carried out. A linear fitting curve with high fitness ($R^2 > 0.99$) and a lower strain measurement error (<15 µε) can be obtained. The aforementioned results make SFBG promising for high-temperature strain sensing in many fields, such as, power plants, gas turbines, and aerospace vehicles.

https://doi.org/10.1364/OL.509397

Strain diagnostics at high temperature is a significant task of structural health monitoring in many fields, such as, power plants, gas turbines, and aerospace vehicles [1–3]. In particular, the high-temperature strain sensor can be applied in a structural health monitoring technology for aerospace vehicles. The thermal protection system (TPS) was employed to keep the underlying structure within acceptable temperature limits and maintain the aerodynamic shape of the vehicle without excessive deformation [4]. During the ascent and reentry stages, the TPS will suffer from the extremely high strain caused by aerodynamic heating (i.e., up to 1000°C) and pressure loads [5]. Hence, to improve the performance of the TPS, a precise strain measurement at high temperature is imperative. It is a great challenge for the traditional welded strain gauges since it only can operate below 350°C [6]. To cover this issue, the platinum based-strain gauges have been proposed, which can withstand high temperature up to 850°C [7].

Moreover, optical fiber-based devices, such as fiber Bragg gratings (FBGs) and Fabry–Perot interferometers (FPIs) have been developed as strain sensors due to their high sensitivity, light weight, compact size, and immunity to electromagnetic interference [8]. The femtosecond laser-inscribed FBGs are ideal devices for monitoring strain at high temperature of up to 1000°C due to the structural changes inscribed using high-intensity laser pulses [9]. However, all silica-based devices will be elongated irreversibly, when a certain strain is applied to the fiber above 800°C. This temperature has reached a softening point of the silica fiber. The pure-silica-core optical fiber may have a higher point, but it is difficult to exceed 1000°C [10].

A single crystal sapphire fiber has a high melting point of ~2045°C, which is much higher than the glass transition temperature of the silica (i.e., 1330°C), and hence could be developed for fabricating strain sensors with higher temperature resistance [11]. To date, two different devices, i.e., FBG and FPI, have been reported [12,13]. For example, sapphire fiber-based intrinsic FPI was proposed for the temperature measurement up to 1510°C [14]. And then, the sapphire fiber air gap-based extrinsic FPI was reported and used for strain and temperature measurement [15]. Both of them exhibit an excellent sensing performance. However, the multiplexing ability of such a FPI structure is limited and is difficult to improve [16].

Sapphire fiber Bragg grating (SFBG) was reported for the first time in 2004 [12], which can operate in high temperature of up to 1500°C or even 1900°C [17]. Moreover, the construction ability of the wavelength-division-multiplexed (WDM) array is enhanced obviously by employing the femtosecond laser

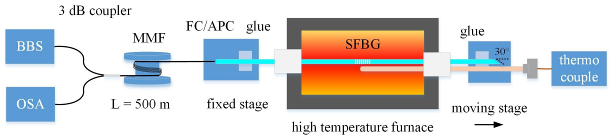

Fig. 1. Schematic setup of SFBG strain sensing experiments at high temperatures. Note that a 500 m length MMF was used to improve wavelength demodulation stability.

direct writing technique, and then the quasi-distributed high-temperature sensing could be realized [18,19]. Furthermore, compared to the FPI, the SFBG contains only the sapphire material without adhesive, exhibiting a higher thermal stability. In 2010, Mihailov *et al*. first reported simultaneous measurement of temperature and strain by using the SFBG and blackbody radiation [20], and then Sun *et al*. used the SFBG to detect strain at 1600°C [21,22], which demonstrates that the SFBG has an excellent strain sensing ability in a harsh environment. A design and packaging of the SFBG based-strain sensors was presented, promoting its practical application [23]. However, the investigation on the long-term stability of the SFBG under high temperature with an applied strain is still missing.

In this paper, we studied experimentally the strain characteristics under high temperatures of femtosecond laser-inscribed SFBG by using an ultrahigh temperature tensile testing system. The changes in topography and the reflection spectra of SFBG under 1600°C with the applied strain indicate that the SFBG was elongated irreversibly. Moreover, the stability in the Bragg wavelength was evaluated when a certain strain was applied to the SFBG under various temperatures. The results show that the SFBG can measure the strain reliably below 1200°C. Furthermore, the high-temperature strain experiments of SFBG at 25°C, 800°C, and 1100°C have been carried out, exhibiting a good sensing performance.

The SFBG was inscribed on a sapphire fiber with a diameter of 100 µm and a length of 40 cm by using the femtosecond laser line-by-line scanning technique [18]. The grating structure was located in the middle of the fiber. The fabrication parameters (i.e., period, pulse energy, scanning velocity, track length, and grating length) were set as 1.76 µm, 30 nJ, 0.1 mm/s, 60 µm, and 2 mm. Moreover, as shown in Fig. 1, the interrogator consists of a customized 1 × 2 105/125 µm multimode fiber coupler (50:50), a broadband light source, and an optical spectrum analyzer (OSA Yokogawa, AQ6370D). Moreover, the launch fiber contributes to the full excitation of the guiding modes in sapphire fibers, resulting in stable and smooth reflection spectra of the SFBG. After optimizing, a 105/125 µm multimode fiber (MMF) with a length of 500 m was selected. Furthermore, to reduce the background intensity and thus increase the signal-to-noise ratio (SNR) of the Bragg reflection peak, the output end of the sapphire fiber was polished to 30° [24]. The input end was polished to 8° (Ferrule Connecter/Angled Physical Contact (FC/APC)). The reflection spectrum of the SFBG was measured by using the above-mentioned setup and is shown together with the broadband light source spectrum in Fig. 2(a), exhibiting a fourth-order Bragg wavelength of 1534.513 nm. Due to the asymmetric multimode reflection peak, the conventional single mode FBG wavelength demodulation method is not suitable. The measured spectrum was processed firstly by using the Savitzky–Golay (SG) filtering and then fitted by using the Gaussian-like function. As shown in Fig. 2(b), the Bragg wavelength was evaluated by using the

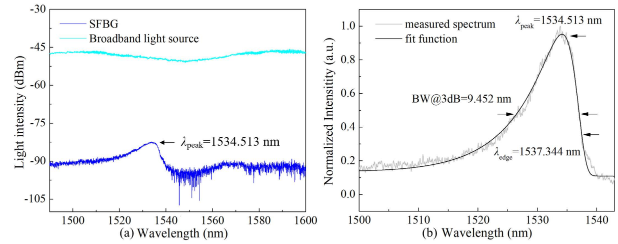

Fig. 2. (a) SFBG reflection spectrum and broadband light source spectrum. (b) Measured reflection spectrum of SFBG and its fit function. λ_{edge} defined as the intersection point of the peak from the fit function with 1/e of its height.

long-wavelength edge detection method, since the fundamental mode (i.e., λ_{edge} = 1537.344 nm) has a more stable transmission performance than high-order modes (i.e., λ_{peak} = 1534.513 nm). Such a demodulation method is beneficial for the enhancement of the stability in the Bragg wavelength searching, referred to in [25].

At first, we investigated the plastic deformation characteristics of the SFBG by using an ultrahigh temperature tensile testing system, as shown in Fig. 1, consisting of a customized universal testing machine (EM1.504-S, TESMART) and a compact high-temperature furnace (THM500, MHI). Note that a B-type thermocouple was placed along the SFBG to record the temperature. The certain strain of 650 µε was applied to the SFBG at room temperature, 1180 and 1600°C for 8 h. The reflection

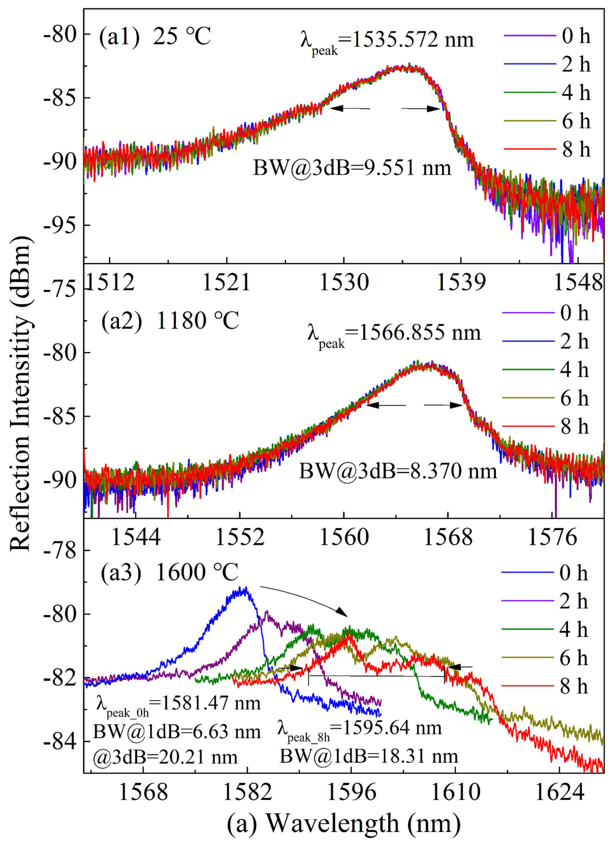

Fig. 3. Long-term stability of SFBG under certain strain at 25°C, 1180°C, and 1600°C. (a1–a3) Evolutions of reflection spectra and (b1–b3) the change in tensile force of the SFBG.

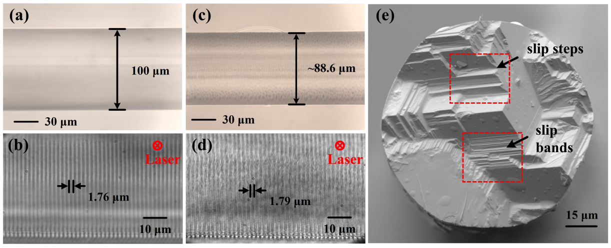

Fig. 4. Certain strain of 650 με was applied to SFBG at 1600°C. Lateral-view microscope and SEM images of SFBG (a), (b) before and (c), (d) after the test. (e) Fracture cross section of SFBG.

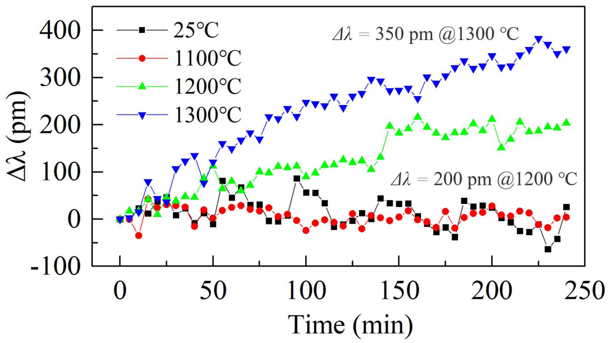

Fig. 5. Evolutions in Bragg wavelength of SFBG at 25°C, 1100°C, 1200°C, and 1300°C with applied 750 με.

spectra were measured and recorded every 5 min. In the case of the 25°C and 1180°C, as shown in Figs. 3(a1) and 3(a2), there is no evident change in the spectral shape of the SFBG. As displayed in Figs. 3(b1) and 3(b2), the tensile force of the SFBG has no significant decrease. However, the reflection peak of the SFBG exhibits a redshift of about 15 nm, and the bandwidth gradually broadens to about 18 nm within 8 h at 1600°C with the applied strain, as illustrated in Fig. 3(a3). Note that, at the same time, the tensile force value decreases by 0.60 N in this process, as shown in Fig. 3(b3). These results indicate that the SFBG cannot operate stably at 1600°C with the applied strain.

Then the topography of the SFBG before and after a high-temperature strain test was observed using an optical microscope and a scanning electron microscope (SEM). As shown in Figs. 4(a), the diameter of the SFBG region decreases from 100 to 88.6 μm, and the grating period is extended from 1.76 to 1.79 μm. These results indicate that the SFBG was elongated irrecoverably after the high-temperature (1600°C) strain test. Given a sapphire fiber dimeter of 100 μm and a strain of 650 με, the stress of the SFBG was calculated as 242 MPa. Unal *et al.* demonstrated that the plastic deformation would happen in c-axially oriented sapphire fibers at 1400°C with an applied stress of 100 MPa [26]. Hence, in our experiment, the irreversible elongation of the SFBG results from plastic deformation.

The glide dislocations of the lattice are determined as a main mechanism of plastic deformation in single crystal materials [27]. To investigate such a mechanism, SFBG was tested at 1600°C with an applied strain of 1000 με, and then the SFBG breaks. Two typical topographies, i.e., slip steps and slip bands can be observed in Fig. 4(e), which indicate that the glide dislocations of the lattice in SFBG happened under a high-temperature stain test [26]. Moreover, as shown in Fig. 3(b3),

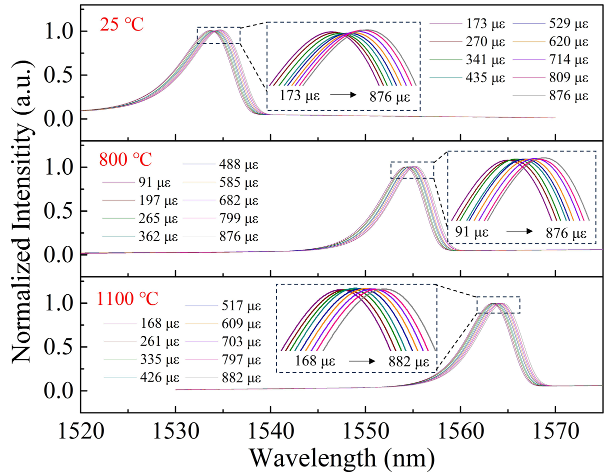

Fig. 6. Evolutions of the SFBG spectrum at 25°C, 800°C, and 1100 °C with applied strain. The fitted spectra are used here, and the insets are a localized enlargement of the reflection peaks.

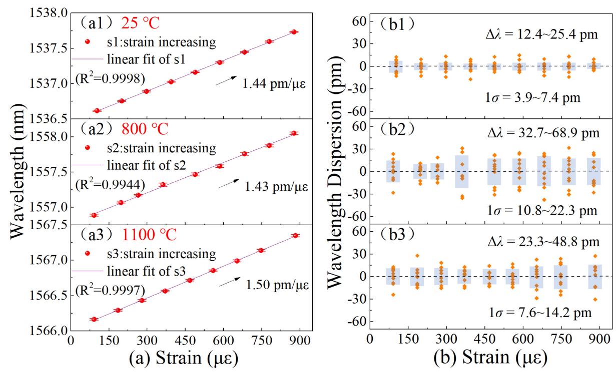

Fig. 7. Strain response of the SFBG at 25°C, 800°C, and 1100°C. (a) Linear fitting relationship between the Bragg wavelength and strain. (b) Dispersion in the Bragg wavelength during strain testing.

a jagged fluctuation in tensile force curve is obvious. This phenomenon is mainly caused by the dislocation-source shutdown [28], where the dislocations are line defects in the sapphire lattice.

To determine the critical temperature point of plastic deformation, the SFBG sample was subjected to 750 με at 25°C, 1100°C, 1200°C, and 1300°C, respectively, and stabilized for 4 h. The reflection spectra were recorded every 5 min. The experimental results were shown in Fig. 5. The Bragg wavelength exhibits a bit fluctuation of about 50 pm for 4 h at 25°C, which is still within the tolerance (i.e., ∼100 pm) of the long-wavelength edge detection method [25]; moreover, there is no redshift trend as displayed in the black curve. In the case of the 1100°C illustrated in the red curve, the Bragg wavelength remained stable which is similar with the case of 25°C. When the temperature increases to 1200°C, as shown in the green curve, the Bragg wavelength has a significant redshift (i.e., 200 pm). In addition, the blue curve exhibits a larger wavelength shift of 350 pm at 1300°C. These results indicate that 1200°C is a critical point of plastic deformation of the sapphire fiber. Hence, the SFBG can be merely applied to measure strain below 1200°C.

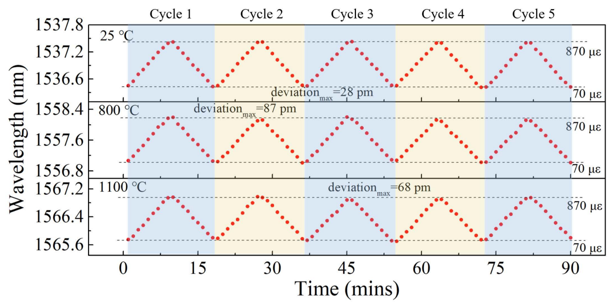

Fig. 8. Measurement cycles of SFBG at 25°C, 800°C, and 1100°C.

The strain response of the SFBG is evaluated at 25°C, 800°C, and 1100°C, respectively. The strain ranging from 0 to 900 με was applied to the SFBG. Ten interval reflection spectra were recorded at each measurement point. As shown in Fig. 6, the corresponding reflection spectra have a large redshift with the increase of 1100°C. When the temperature is stable at 25°C, 800°C, and 1100°C, the Bragg peak exhibits a regular redshift with the strain increasing, as displayed in the insets of Fig. 6. Then the corresponding Bragg wavelengths were determined by using the long-wavelength edge detection method. Figures 7(a1)–7(a3) show the relationship between the Bragg wavelength and the strain at different temperatures. By using the linear fitting function, all of the three curves with high fitness ($R^2 > 0.99$) are realized. The strain sensitivities at 25, 800, and 1100°C are 1.44, 1.43, and 1.50 pm/με, respectively, which are close to the other published data [21–23]. As shown in Figs. 7(b1)–7(b3), the maximum wavelength dispersions of the strain test under three temperature points are 25.4, 68.9, and 48.8 pm, respectively. The corresponding one σ error bar are 7.4, 22.3, and 14.2 pm, which indicates that the SFBG has a lower strain measurement error (<15 με) below 1200°C. It should be noted that the wavelength dispersions at 800 and 1100°C are larger than that at 25°C, since the temperature of furnace has a bit fluctuation (i.e., ±1°C). Moreover, to study the repeatability of the strain sensing response of the SFBG, five measurement cycles have been performed at 25°C, 800°C, and 1100°C. As shown in Fig. 8, in the case of 25°C, the maximum deviation of the Bragg wavelength is 28 pm at the end of the second cycle, corresponding to ~20 με, which exhibits preferable repeatability. Moreover, the maximum deviation values increase to 87 and 68 pm at 800°C and 1100°C, respectively, caused by fluctuation of the temperature in the furnace (i.e., ±1°C). The temperature sensitivity of the SFBG is 29.8 pm/°C at 800°C, corresponding to the ~60 pm fluctuation [19].

In this work, we have reported for the first time to our knowledge on the critical temperature point of plastic deformation of SFBG, determining the long-term stability of SFBG at high temperature with an applied strain. The effects of high-temperature applied tensile on the topography and the reflection spectra of the SFBG have been investigated. The reflection peak of the SFBG shows a significant redshift of about 15 nm and broadens gradually within 8 h at 1600°C with the applied strain, and the tensile force value decreases by 0.60 N. After the test, a 100 μm diameter SFBG is obviously thinner (i.e., 88.6 μm), and the original grating period of 1.76 μm increases to 1.79 μm. These indicate that the SFBG has been elongated irreversibly in this process. Moreover, a series of tensile tests under various temperatures ranging from 25°C to 1300°C were carried out. The experimental results demonstrate SFBG can operate stably below 1200°C. Furthermore, the strain sensing responses of SFBG at various temperatures of 25°C, 800°C, and 1100°C have been tested. A linear fitting curve with high fitness ($R^2 > 0.99$) and a lower strain measurement error (<15 με) can be obtained. Therefore, such a SFBG exhibits a reliable high-temperature strain sensing performance, which can be applied for structural health monitoring in many fields, such as power plants, gas turbines, and aerospace vehicles.

Funding. National Natural Science Foundation of China (NSFC) (62222510, 62375176); National Key Research and Development Program of China (2023YFB3208600); Science and Technology Innovation Commission of Shenzhen (RCYX20200714114538160); Shenzhen Key Laboratory of Ultra-fast Laser Micro/Nano Manufacturing (ZDSYS20220606100405013) (2022B1515120050); Science, Technology and Innovation Commission of Shenzhen Municipality (20220810164735001, RCYX20200714114538160, ZDSYS20220606100405013); LingChuang Research Project of China National Nuclear Corporation (CNNC-LCKY-202259).

Disclosures. The authors declare no conflicts of interest.

Data availability. Data underlying the results presented in this paper are not publicly available at this time but may be obtained from the authors upon reasonable request.

REFERENCES

1. D. Sziroczak and H. Smith, Prog. Aeronaut. Sci. **84**, 1 (2016).
2. G. Locatelli, M. Mancini, and N. Todeschini, Energy Policy **61**, 1503 (2013).
3. M. Tahan, E. Tsoutsanis, M. Muhammad, *et al.*, Appl. Energy **198**, 122 (2017).
4. G. Xie, Q. Wang, B. Sunden, *et al.*, Appl. Therm. Eng. **59**, 425 (2013).
5. V. Le, N. S. Ha, and N. S. Goo, Composites, Part B **226**, 109301 (2021).
6. P. Schmid, C. Zarfl, G. Balogh, *et al.*, Procedia Eng. **87**, 172 (2014).
7. S. Fricke, A. Friedberger, G. Mueller, *et al.*, *Sensors, 2008 IEEE* (IEEE, 2008), pp. 1532–1535.
8. Z. Ran, X. He, Y. Rao, *et al.*, Photonic Sens. **11**, 227 (2021).
9. J. He, B. Xu, X. Xu, *et al.*, Photonic Sens. **11**, 203 (2021).
10. Y. Zhang, X. Ding, Y. Song, *et al.*, Meas. Sci. Technol. **29**, 035102 (2018).
11. R. R. Dils, J. Appl. Phys. **54**, 1198 (1983).
12. D. Grobnic, S. J. Mihailov, C. W. Smelser, *et al.*, IEEE Photonics Technol. Lett. **16**, 2505 (2004).
13. A. Wang, S. Gollapudi, K. A. Murphy, *et al.*, Opt. Lett. **17**, 1021 (1992).
14. A. Wang, S. Gollapudi, R. G. May, *et al.*, Opt. Lett. **17**, 1544 (1992).
15. A. Wang, S. Gollapudi, and R. G. May, Smart Mater. Struct. **4**, 147 (1995).
16. J. Wang, B. Dong, E. Lally, *et al.*, Opt. Lett. **35**, 619 (2010).
17. T. Habisreuther, T. Elsmann, Z. Pan, *et al.*, Appl. Therm. Eng. **91**, 860 (2015).
18. X. Xu, J. He, C. Liao, *et al.*, Opt. Lett. **43**, 4562 (2018).
19. X. Xu, J. He, J. He, *et al.*, Opt. Lett. **46**, 2742 (2021).
20. S. J. Mihailov, D. Grobnic, and C. W. Smelser, Opt. Lett. **35**, 2810 (2010).
21. C. Chen, X. Zhang, and Y. Yu, J. Lightwave Technol. **36**, 3302 (2018).
22. Q. Guo, Y. Yu, Z. Zheng, *et al.*, IEEE Trans. Nanotechnol. **18**, 208 (2019).
23. T. Habisreuther, T. Elsmann, A. Graf, *et al.*, IEEE Photonics J. **8**, 1 (2016).
24. G. Shi, R. Shurtz, G. Pickrell, *et al.*, Opt. Lett. **47**, 4724 (2022).
25. R. Eisermann, S. Krenek, T. Habisreuther, *et al.*, Sensors **22**, 1034 (2022).
26. O. Unal, K. P. D. Lagerlof, and G. S. Corman, Ceram. Eng. Sci. Proc. **14**, 600 (1993).
27. S. Deng, J. Mater. Sci. **31**, 6077 (1996).
28. H. Tang, K. W. Schwarz, and H. D. Espinosa, Phys. Rev. Lett. **100**, 185503 (2008).